photonics

MDPI

Article

Spectral Self-Compression of Chirp-Free Pulses in Anomalously Dispersive Optical Fibers

Minas Sukiasyan [1,2,*], Vardan Avetisyan [1] and Aghavni Kutuzyan [1]

[1] Ultrafast Optics and Photonics Laboratory, Faculty of Physics, Yerevan State University, 1 Alex Manoogian Street, Yerevan 0025, Armenia; vardan.avetisyan1@ysu.am (V.A.); akutuzyan@ysu.am (A.K.)
[2] Candle Synchrotron Research Institute, Yerevan 0022, Armenia
* Correspondence: minas.suqiasyan@ysu.am

Abstract: In this work, we demonstrated, both experimentally and numerically, the existence of a chirp-free pulse propagation regime within a standard single-mode fiber. We found numerically that the pulse spectrum can undergo self-compression by more than a hundredfold, resulting in the creation of a spectrally limited pulse. In this regime, we experimentally achieved a 5× spectral self-compression, reducing the spectral width from 75 nm to 15 nm within the 1.3–1.5 µm spectral range. This was achieved with a standard telecommunication fiber with constant dispersion.

Keywords: fiber optics; temporal solitons in fibers; spectral compression; soliton self-forming process; group velocity dispersion

1. Introduction

Nonlinear spectral compression (SC) [1–4], which is particularly interesting for developing telecommunication fiber communication lines [5] and building efficient fiber amplifiers [6], is full of promising applications in ultrafast optics and laser physics. In contrast to linear spectral filtering, which discards frequency components beyond the specified region of the spectrum, the nonlinear SC process concentrates the energy of the pulse around the central wavelength without losing energy.

The standard technique for SC involves the following two components: a medium with a negative dispersion to create a negatively chirped pulse and a medium with positive cubic nonlinearity to compress the spectrum [2–4]. As a medium with a negative dispersion, dispersive delay lines are primarily used, such as negative chirped mirrors, pairs of diffraction gratings, prisms, etc. An optical fiber is predominantly utilized as a medium with positive cubic nonlinearity. The propagation of a negatively chirped pulse in a fiber with cubic nonlinearity results in chirp compensation and the occurrence of SC. In the fiber, compression is achieved by self-phase modulation (SPM) [1], which transfers energy from the wings of the spectrum toward its central part. SC has been demonstrated using different types of fibers and wavelengths [6–15]. In particular, in the past few years, SC has been demonstrated using photonic crystal fibers with dispersion-increasing structures [8,9], optical gain fibers [6,12,13], comb-profile fibers [14,15], etc.

SC with the standard technique is experimentally demonstrated in all-fiber schemes without a classic dispersive delay line. In particular, the authors of [16] conducted a comparative analysis of different methods for SC using the Ti:Saphire laser system. The SC of femtosecond pulses is demonstrated through classical, all-fiber, and similaritonic techniques. In the classical scheme, a 12× SC was achieved by utilizing a pair of prisms as a dispersion delay line. In the all-fiber technique, hollow-core fiber was used as dispersion mediawhich has negative dispersion at the central wavelength of the laser. Using this approach, an 8.4× SC was obtained. The similaritonic method was employed to achieve a higher degree of SC without any aberrations. This was achieved by compensating the phase of the dispersion medium with the phase of a similariton pulse in the process of

check for updates

Citation: Sukiasyan, M.; Avetisyan, V.; Kutuzyan, A. Spectral Self-Compression of Chirp-Free Pulses in Anomalously Dispersive Optical Fibers. *Photonics* **2023**, *10*, 1207. https://doi.org/10.3390/photonics10111207

Received: 2 September 2023
Revised: 13 October 2023
Accepted: 27 October 2023
Published: 29 October 2023

sum-frequency generation. In the results, a 23× SC was achieved. To use the optical fibers in the standard technique of SC requires attention not only to nonlinearity but also to group velocity dispersion (GVD).

It is known that GVD in fibers is not detrimental. Moreover, it plays an important role in the SC process, in particular in terms of its value and sign. For instance, in the standard technique of SC with normal GVD influence, near-transform-limited rectangular and parabolic pulses are generated in the regime of optimum compression [17–20]. On the other hand, the combination of anomalous GVD and positive cubic nonlinearity allows for having SC in a single medium, such as a fiber. Based on this approach, in [14,19], the authors obtained SC in a dispersion-increasing fiber (DIF) without an initial negative chirp at the expense of soliton propagation. Nishizawa et al. initially introduced the concept of using DIF for SC in their work [14]. This method made it possible to increase the extent of SC for ultrashort laser pulses. The utilization of a DIF allows for the achievement of an SC across a broad spectrum of wavelengths based on the adiabatic soliton SC technique. This approach to SC is the spectral analogue of adiabatic soliton compression (ASC), which allows reaching chirp-free pulse compression without applying high-order soliton compression. In particular, the authors of [20] achieved pulse compression at 2 μm using a two-stage APC technique, reducing the pulse duration from 130 fs to 15 fs. In this context, a gas-filled pressure-gradient hollow-core fiber is employed to mitigate pedestal effects and improve the quality of the compressed pulse.

With this approach to SC, the researchers in [21] utilized a fiber with a length of 0.8 km, featuring exponentially increasing dispersion. As a result of soliton propagation, they successfully obtained a 10× SC without the requirement for an initial chirped pulse. The authors also demonstrated that a smaller initial pulse width, a larger value of the initial dispersion, and a smaller exponentially increasing rate of dispersion are needed to obtain better SC for transforming limited Gaussian or hyperbolic secant pulses.

The authors of [19] experimentally obtained the largest SC coefficient of 102.8×, which is based on that approach. In conjunction with SC, the authors also demonstrated that the spectrally compressed peak wavelength is tunable from 1578.5 nm to 1695 nm.

The research interest in this field advances because it opens up a new opportunity for the development of laser sources with tunable wavelengths. Recently, the authors of [22] presented an all-fiber, amplified narrow-linewidth laser source, which is based on the SC of wavelength-shifted femtosecond pulses. In this work, the DIF fiber was used, which is designed based on the comb-like dispersion-profiled fiber (CPF). A 37.2× SC was obtained in the tunable wavelength range of 1622 nm to 1900 nm. This is the best result in this wavelength region.

The effect of negative dispersion and SPM allows for obtaining the SC of chirp-free pulses in fibers with constant dispersion [7,23–25]. The authors of [7] demonstrated SC of chirp-free, diode-pumped ytterbium solid-state laser pulses using an anomalously dispersive photonic crystal fiber (PCF). In this mode, a 2.6× spectral compression was obtained at 30 cm PCF when the input pulse energy was 70 pJ. Furthermore, it was shown that the amount of SC increases as the input power decreases.

In our earlier work, we experimentally demonstrated an SC of 30% at 800 nm wavelength in a hollow-core fiber (HCF) [23]. We also enhanced the SC up to 4.1× at 1400 nm wavelength in a 600 m long single-mode fiber (SMF) [25]. We have shown that the SC process requires a strong GVD and weak nonlinearity in fiber.

In this paper, we present a detailed analysis of the SC of chirp-free pulses in a 900 m long SMF with constant dispersion. Our analysis involves both experimental as well as numerical studies. We call this SC technique self-spectral compression (self-SC). This regime of pulse propagation is interesting and unique; however, it has not been thoroughly studied yet.

2. Analytical Discussion of Self-SC in Anomalously Dispersive Fibers

An important feature of self-SC is that it does not require negatively chirped input pulses. It is based on the mechanism of self-formation and stabilization of the fundamental soliton process. As known from [1], the soliton order N is given as follows:

$$N^2 = \frac{\gamma P_0 T_0^2}{|\beta_2|}, \tag{1}$$

where γ is the nonlinear coefficient, P_0 is the peak power, T_0 is the width of the initial pulse, and β_2 is the second-order dispersion coefficient. It is known that the Nth-order soliton can form when the input value of N is in the range of $N - 0.5$ to $N + 0.5$. In particular, the fundamental soliton ($N = 1$) can be formed for values of N in the range of 0.5–1.5. In addition, a fundamental soliton with an amplitude of $1 + 2a$ is formed from an input pulse with an amplitude of $1 + a$ ($|a| < 0.5$) [26]. In the initial stage of self-shaping, the pulse modification starts with pulse compression and spectrum broadening, or vice versa, depending on the value of N. For values of N in the range of $0.5 < N < 1$, the self-forming process begins with pulse broadening and SC. In the case of $1 < N < 1.5$, we have the opposite physical pattern [1,23,24]. Similar behavior is observed when the input pulse has a non-hyperbolic secant profile (e.g., Gaussian) and $N = 1$. In that case, the pulse adjusts its shape and width in an attempt to become a fundamental soliton and attains a hyperbolic secant profile. In both of these cases, the physical pattern of the fundamental soliton's self-formation has a periodic character; it proceeds with successive compression and stretching of the pulse and its spectrum.

We studied the fundamental soliton formation process in the region of $0.5 < N < 1$ from the point of view of self-SC.

3. Numerical Study

In order to obtain a complete physical pattern of the process and to reveal its typical peculiarities and general regulations, we carried out a numerical study based on the solution of the nonlinear Schrödinger equation (NLSE). As known from [27], when investigating pulse propagation within a medium characterized only by GVD and SPM, NLSE takes the following form:

$$i\frac{\partial \Psi}{\partial \zeta} = \frac{1}{2}\frac{\partial^2 \Psi}{\partial \eta^2} + R|\Psi|^2\Psi, \tag{2}$$

where $\zeta = z/L_D$ is the dimensionless propagation distance normalized to the dispersive length $L_D \equiv 1/\left(\beta_2 \Delta\omega_0^2\right)$, $\Delta\omega_0$ is the spectral bandwidth of the initial spectra, $\eta = (t - z/u)/T_0$ is the "running" time, normalized to the initial pulse duration T_0, $R = \frac{L_D}{L_{NL}}$ is the nonlinearity parameter, where $L_{NL} \equiv \left(\beta_0 n_2 I_0^2\right)^{-1}$ is the nonlinearity length, n_2 is the nonlinear Kerr coefficient, and I_0 is the peak intensity. We used the split-step Fourier method during the numerical solution of the equation with the fast Fourier transform algorithm on the dispersive step [28,29].

The results of our numerical studies for initial Gaussian pulses are depicted in Figure 1. The propagation processes of a pulse and its spectrum for $N = 0.9$ are shown in Figure 1a,b, respectively. The propagation coordinate ζ, in units of the dispersive length L_D, is represented on the horizontal axis. These two figures show the periodic nature of this process associated with high-order solitons. Throughout the propagation process, it is important to note that the chirp change also exhibits periodic behavior. In the first stage of propagation, it assumes a negative value, followed by a positive one, and this alternation continues in a recurring pattern.

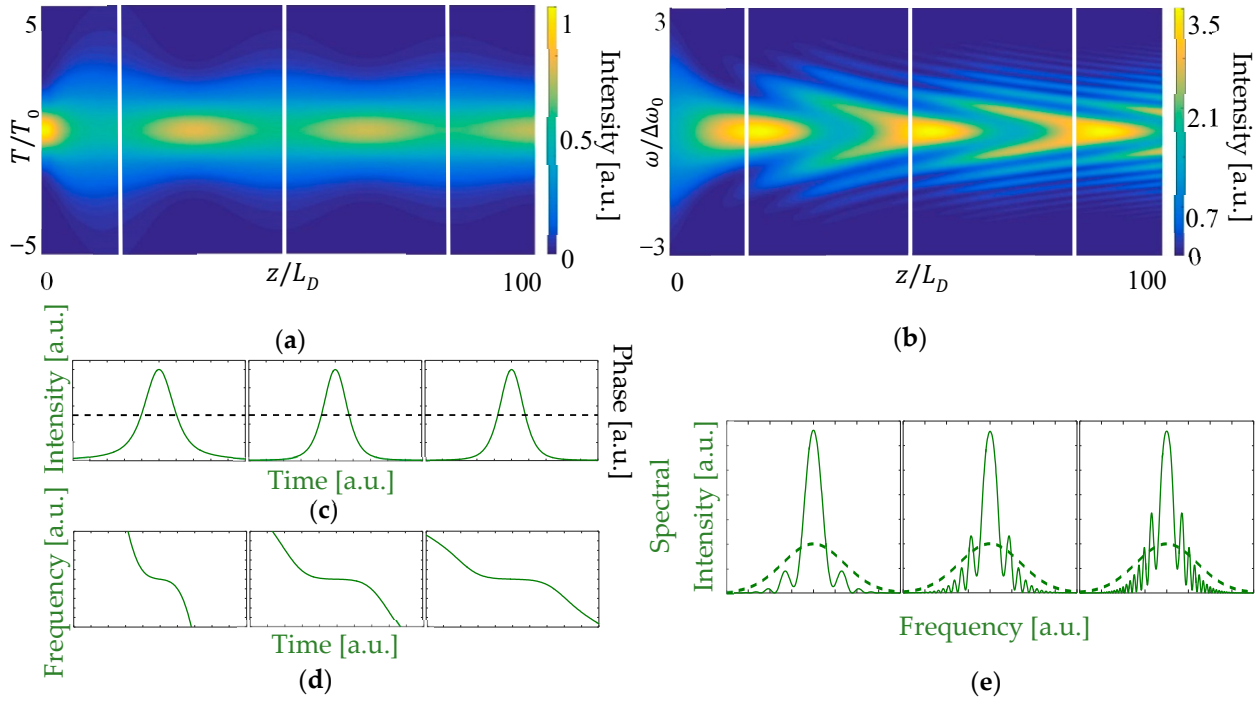

Figure 1. Calculated evolutions of self-SC for a chirp-free Gaussian pulse: 3D dynamics of (**a**) a pulse and (**b**) its spectrum propagation, (**c**) self-expanded pulses (green curves) with their phases (black dotted curves), (**d**) chirps, and (**e**) self-compressed (solid curve) and initial (dotted curve) spectra at z/L_D = 11, 46, and 81 when the GVD-induced chirp is counteracted by the SPM-induced one.

In the initial propagation step (the first white line, at $z/L_D = 11$), the pulse is stretched and the spectrum is compressed. The original temporal form and spectrum of high-order soliton are restored throughout propagation at multiple distances during the soliton period. However, because of incomplete chirp cancellation, the spectral bandwidth at each next maximum compression point is smaller than at the previous one.

We computed the spectral compression ratio, defined as $SCR = \Delta\omega/\Delta\omega_0$, where $\Delta\omega$ is the spectral bandwidth of the compressed spectrum. In particular, at the first, second, and third compression points ($z/L_D = 24.8,\ 54,\ 83$), the *SCR* was 4.5, 5.1, and 5.3, respectively. The quality of self-SC at every next compression point is worse than at the previous one; some fraction of the pulse energy travels to spectral satellites.

The 2D subplots in Figure 1 show the temporal intensity and phase profiles (c), chirp profiles (d), and spectral intensity profiles (e) at the chirp compensation points (z/L_D= 11, 46, 81). In Figure 1c, the green curves represent the temporal profiles, while the black dashed curves depict the phases. Figure 1d indicates that the chirp is compensated by the entire pulse, not just the energy-consuming part. In other words, a near-transform-limited pulse is formed. Within Figure 1e, the solid curves represent the compressed spectrum, while the dotted curves depict the initial spectrum. This process is very similar to the SC dispersion regime in standard SC techniques, where pulses with rectangular envelopes are formed in the region of optimal SC [16]. As it can be seen from the picture, the points of chirp compensation do not coincide with the points of maximum SC. Nevertheless, at those points, there is still self-SC, *SCR* is found to be 2.71, 3.44, and 4, and the pulse stretching coefficient is 2.48, 2, and 1.9, respectively.

The process is different from soliton compression due to the fact that the spectrum depends on a nonlinear phase, which, in turn, depends on the shape of the pulse. The dispersive phase of a soliton has a major impact on the shaping of the pulse throughout its propagation. However, the dispersive phase has no dependence on the shape of the pulse or its spectrum.

The change in the spectrum takes place at a constant period; the maximum compressions or extensions occur at the same distances.

Our calculations show that the nature of the propagation of the pulse is the same for different (Gaussian, hyperbolic secant) pulses. However, the *SCR* and the period are different depending on the shape of the pulse.

The pulse and spectrum peaks versus the dimensionless length of the optical fiber for the initial Gaussian pulse are demonstrated in Figure 2a,b, respectively. The peak intensity of the pulse undergoes a large change in the first stage of propagation in the fiber (as shown in Figure 2(a1)). At each successive pulse compression point, the maximum peak intensity becomes even smaller than the previous one. Nonetheless, as the pulse propagates, the gradual reduction in peak intensity progressively decelerates, eventually stabilizing at a certain value. As represented in Figure 2(a2), the peak intensity is observed to vary less than 0.01% over the final 100 L_D distance.

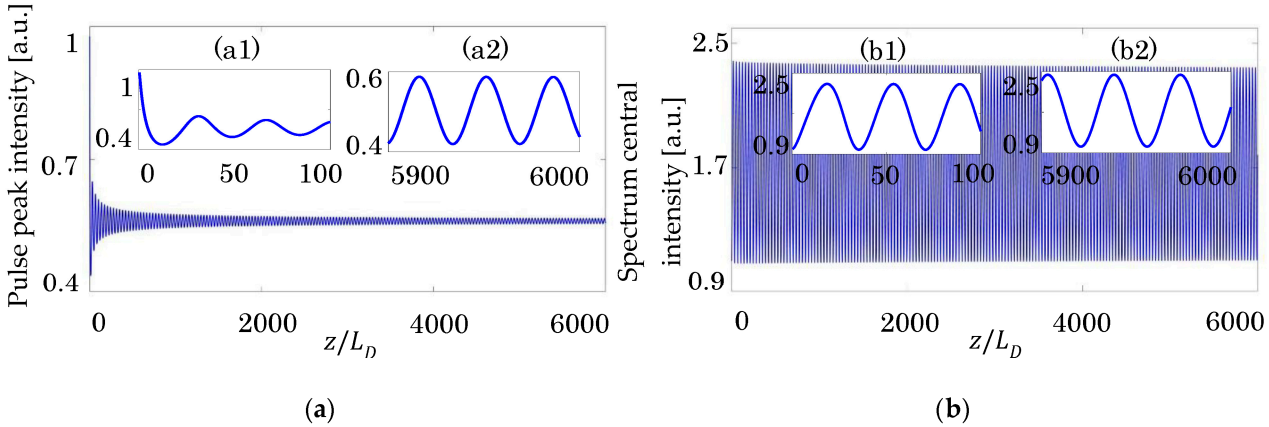

Figure 2. The pulse peak intensity for the: (**a**) whole propagation length, (**a1**) initial (0–100) propagation distance, (**a2**) final (5900–6000) distance and central intensity of the spectrum vs fiber length for the: (**b**) whole propagation, (**b1**) initial (0–100) distance, (**b2**) final (5900–6000) distance. Shown results are computed for a Gaussian initial pulse (N = 0.9).

As we can see from Figure 2b, the central peak intensity of the spectrum repeats the exact value of the first compression at successive compression points.

In our numerical study, we also computed the first compression points (periods) of the self-SC and *SCR* for Gaussian pulses with different values of soliton order N, which are presented in Table 1. It makes the results more practical from an application point of view and useful for process optimization.

It should be noted that the first compression takes place on a shorter length of fiber than the period, which can be seen in Figure 2. Here, the first compression occurs at a length of 18.5 L_D, whereas the period is z_p = 36 L_D. The relationship between the period and soliton order N is visually represented in Figure 3a, and Figure 3b illustrates the dependency of the *SCR* on N. As can be seen from Figure 3a, the period of the process decreases with increasing soliton order N. To increase the *SCR*, it is necessary to reduce the value of N (Figure 3b).

Table 1. Self-SC coefficient (*SCR*) and first compression points (periods) for different values of soliton order (*N*).

N	SCR	Period
0.64	100	11,710
0.65	63	3532
0.66	44	1751
0.67	33.8	985
0.7	19	314
0.75	11	100
0.8	7.7	49
0.85	5.7	28.3
0.9	4.5	24.8
0.95	3.5	13

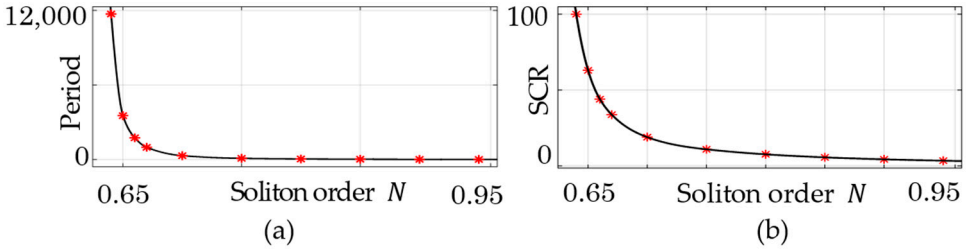

Figure 3. (**a**) First compression points (periods) z/L_D vs. soliton order N; (**b**) SCR vs. soliton order N for the Gaussian pulse.

The approximation of the curve led to the following formula:

$$SCR = \frac{1.532}{N - 0.624} \tag{3}$$

The above dependence of the *SCR* on N allows us to expect that the largest self-SC occurs for values of N close to 0.624. Furthermore, the repetition period of the process increases significantly (Figure 3a) for those values of N. The process of propagation loses its periodic nature for values of N less than or equal to 0.624. In that range of N, a new type of similariton pulse is formed [30]. However, in our studies, we found more than 100× compression in that range. In particular, Figure 4 shows the compressed spectrum for N = 0.64, in which the value of *SCR* is 95.5× and the amount of pulse extension is only 60× for the Gaussian pulse.

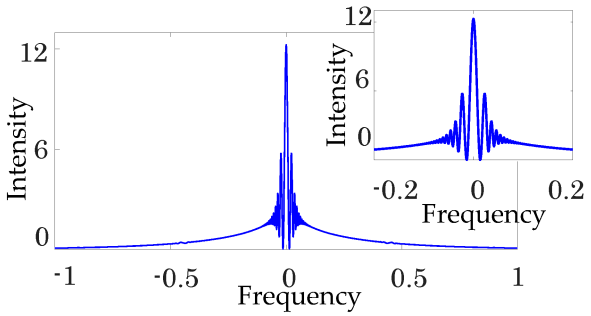

Figure 4. The 95.5× spectral self-compressed spectra of initial Gaussian pulses (N = 0.64, L_D = 11,700).

4. Experiment

4.1. Experimental Setup

The experiment was performed using an amplified Yb:YAG laser system (Amplitude Systems), which delivered 400 fs at 1030 nm pulses with an energy of up to 2 mJ at a 1 kHz repetition rate. Figure 5a shows the schematic diagram of the experiment. Self-SC was experimentally demonstrated in a standard single-mode telecommunication optical fiber (SMF). To reach the wavelength region of 1300 nm and above, where silica has negative GVD, we generated a supercontinuum [31–34]. In order to generate a supercontinuum, we employed an yttrium aluminum garnet (YAG) crystal, which is an excellent nonlinear medium with a high optical damage threshold, a good crystalline quality, and a high nonlinearity. The laser output beam was varied by a combination of a high-power polarizing beam-splitter cube (PBS25-1064-HP from Thorlabs) and a half waveplate. A selection of the input energy range was made to avoid optical damage to the crystal. To create a supercontinuum, the laser beam was focused by a Plano convex lens with a +3 cm focal length onto the input face of the 7 mm long YAG crystal, which was positioned at the lens's focal plane. With an input pulse energy of ~20 µJ, the supercontinuum spectrum extends from 800 nm to 1550 nm, as shown in Figure 5b. After the generation, the spectrum was cut with a hard-coated IR long-pass filter (FELH1300 from Thorlabs) at 1300 nm, as shown in Figure 5c. After cutting the spectrum, we coupled the beam into a 900 m long SMF. The optimal SC for the specified length of the fiber was achieved by controlling the input power with a continuously variable neutral density filter (NDC-50C-2M from Thorlabs).

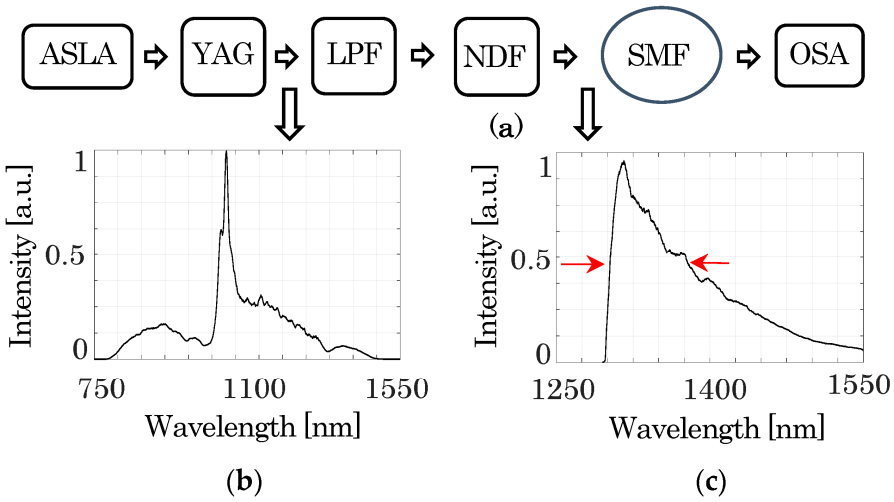

Figure 5. (Color online) (**a**) Schematic experimental setup: ASLA: amplitude system laser + amplifier; YAG: yttrium aluminum garnet crystal; LPF: long-pass filter; NDF: neutral density filter; SMF: conventional single-mode telecom fiber; OSA: optical spectrum analyzer. (**b**) Supercontinuum spectrum of the YAG crystal output. (**c**) Supercontinuum spectrum cut at 1300 nm.

4.2. Results and Discussion

The spectral measurements were performed using an optical spectrum analyzer (Ando AQ-6315A) with a 10 nm resolution. The spectral bandwidth was 75 nm at the input of the fiber (the cut spectrum was used as the initial spectrum), as shown in Figure 5c. The spectral profiles at the output of the 900 m SMF are shown in Figure 6 for average radiation powers of 0.8 mW (a), 1 mW (b), and 1.6 mW (c). Power measurements were performed using a pyroelectric energy sensor, the PE10-C model from Ophir.

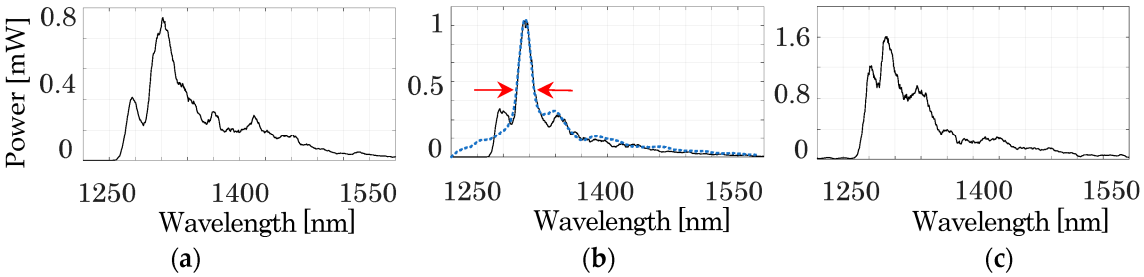

Figure 6. Experimental and numerical demonstrations of self-SC. Experimental (black curves) and numerical (blue dotted curve) spectral profiles of ultrashort pulses at the output of a 900 m long fiber for (**a**) 0.8 mW, (**b**) 1 mW, and (**c**) 1.6 mW average powers.

At a power level of 0.8 mW (as shown in Figure 6a), the degree of spectral narrowing does not exceed twice its initial size ($\Delta\lambda \approx 40$ nm, where $\Delta\lambda$ is the spectral bandwidth at FWHM of the compressed spectra). Based on the results of numerical simulations (as shown in Figure 1b), it can be inferred that this point corresponds to a position prior to achieving optimal compression. With an increase in input power, the level of self-SC also rises. At the power of 1 mW, a five-times self-SC is obtained, where $\Delta\lambda \approx 15$ nm (as shown in Figure 6b). With a further increase in the radiation power (at 1.6 mW), the amount of self-SC decreases (as shown in Figure 6c). The optimal fivefold self-SC is attained when the power level reaches 1 mW.

Due to the inherent noisy nature of the supercontinuum, we conducted a numerical analysis to explore the propagation of randomly modulated pulses in the medium with negative dispersion and nonlinearity [30]. For the noisy pulse, we employed the "regular pulse + noise" model. As a regular pulse, we used secant hyperbolic pulses. We examined pulses with amplitude modulation, phase modulation, and both amplitude and phase modulation combined. In the case of both regular and noise pulses, the phenomenon of self-supercontinuum (self-SC) occurs; however, the amount of spectral broadening and the compression period depend on the amplitude of the noise.

We also performed numerical simulations of self-SC using the spectrum from Figure 5c as the initial spectrum. The results were in good agreement with the experimental results (Figure 6b). Similar numerical studies were already carried out in [21]. Note that the broadened spectra are symmetric, which suggests that the influence of high-order dispersion and nonlinear effects on SC is absent for these parameters of the system. The study shows that the self-SC cleans out the pulse by suppressing the noise.

Hence, our experimental results provide clear evidence of the potential of self-SC in noise-type pulses. The obtained results were limited by the value of the crystal damage threshold, preventing us from accessing the extended wavelength range of the spectrum (1600 and more). This limitation ultimately prevented us from achieving higher compression values.

5. Conclusions

Based on our experimental and numerical studies, we investigated the nonlinear phenomenon of self-SC, which can be seen as the spectral equivalent of soliton compression. We revealed the nature and general features of self-SC, which can serve to optimize the process. We demonstrated that the nonlinear self-SC phenomenon occurs when the dispersion expansion of the pulse proceeds faster than the change of its spectrum as a result of SPM in the fiber with negative dispersion.

Through our numerical analysis, we showed a high level of self-SC for a chirp-free Gaussian pulse, exceeding a hundredfold.

We have experimentally demonstrated a 5× self-SC of a noisy supercontinuum spectrum in a 900 m single-mode fiber in the 1300 nm–1500 nm spectral region. Our experimental data were compared to numerical calculations and were all found to be in good agreement.

Additionally, our investigations covered a broad range of long wavelengths in the supercontinuum generation, which is of great importance for applications in nonlinear microscopy, optical coherence tomography, and metrology.

Author Contributions: Conceptualization, M.S. and A.K.; methodology, A.K.; software, M.S., V.A. and A.K.; validation, A.K.; formal analysis, M.S., V.A. and A.K.; investigation, M.S. and A.K.; resources, A.K. and V.A.; data curation, M.S. and V.A.; writing—original draft preparation, M.S. and V.A.; writing—review and editing, A.K.; visualization, M.S. and V.A.; supervision, A.K.; project administration, A.K.; funding acquisition, M.S. and A.K. All authors have read and agreed to the published version of the manuscript.

Funding: This work was supported by the Science Committee of RA (Research project No 10-3/23-I/YSU-PHYS).

Institutional Review Board Statement: Not applicable.

Informed Consent Statement: Not applicable.

Data Availability Statement: Not applicable.

Conflicts of Interest: The authors declare no conflict of interest.

References

1. Agrawal, G.P. *Nonlinear Fiber Optics*, 6th ed.; Academic Press: Cambridge, MA, USA; Elsevier Science: Amsterdam, The Netherlands, 2019.
2. Markaryan, N.L.; Muradyan, L.K.; Papazyan, T.A. Spectral compression of ultrashort laser pulses. *Sov. J. Quantum Electron.* **1991**, *21*, 783–785. [CrossRef]
3. Oberthaler, M.; Hopfel, R.A. Special narrowing of ultrashort laser pulses by self-phase modulation in optical fibers. *Appl. Phys. Lett.* **1993**, *63*, 1017–1019. [CrossRef]
4. Planas, S.A.; Pires Mansur, N.L.; Brito Cruz, C.H.; Fragnito, H.L. Spectral narrowing in the propagation of chirped pulses in single-mode fibers. *Opt. Lett.* **1993**, *18*, 699–701. [CrossRef]
5. Cundiff, S.T.; Collings, B.C.; Boivin, L.; Nuss, M.C.; Bergman, K.; Knox, W.H.; Evangelides, S.G. Propagation of Highly Chirped Pulses in Fiber-Optic Communications Systems. *J. Light. Technol.* **1999**, *17*, 811–815. [CrossRef]
6. Limpert, J.; Gabler, T.; Liem, A.; Zellmer, H.; Tünnermann, A. SPM-induced spectral compression of picosecond pulses in a single-mode Yb-doped fiber amplifier. *Appl. Phys. B* **2002**, *74*, 191–195. [CrossRef]
7. Sidorov-Biryukov, D.A.; Fernandez, A.; Zhu, L.; Pugzlys, A.; Serebryannikov, E.E.; Baltuska, A.; Zheltikov, A.M. Spectral narrowing of chirp-free light pulses in anomalously dispersive, highly nonlinear photonic-crystal fibers. *Opt. Express* **2008**, *16*, 2502–2507. [CrossRef]
8. Andresen, E.R.; Thøgersen, J.; Keiding, S.R. Spectral compression of femtosecond pulses in photonic crystal fibers. *Opt. Lett.* **2005**, *30*, 2025–2027. [CrossRef]
9. Chuang, H.P.; Huang, C.B. Wavelength-tunable spectral compression in a dispersion-increasing fiber. *Opt. Lett.* **2011**, *36*, 2848–2850. [CrossRef] [PubMed]
10. Fatome, J.; Kibler, B.; Andresen, E.R.; Rigneault, H.; Finot, C. All-fiber spectral compression of picosecond pulses at telecommunication wavelength enhanced by amplitude shaping. *Appl. Opt.* **2012**, *51*, 4547–4553. [CrossRef]
11. Limpert, J.; Deguil-Robin, N.; Manek-Hönninger, I.; Salin, F.; Schreiber, T.; Liem, A.; Röser, E.; Zellmer, H.; Tünnermann, A.; Courjaud, A.; et al. High-power picosecond fiber amplifier based on nonlinear spectral compression. *Opt. Lett.* **2005**, *30*, 714–716. [CrossRef]
12. Rusu, M.; Okhotnikov, O.G. All-fiber picosecond laser source based on nonlinear spectral compression. *Appl. Phys. Lett.* **2006**, *89*, 091118. [CrossRef]
13. Bao, C.; Xiao, X.; Yang, C. Spectral compression of a dispersion managed mode-locked Tm: Fiber laser at 1.9 μm. *IEEE Photon. Technol. Lett.* **2015**, *28*, 497–500. [CrossRef]
14. Nishizawa, N.; Takahashi, K.; Ozeki, Y.; Itoh, K. Wideband spectral compression of wavelength tunable ultrashort soliton pulse using comb profile fiber. *Opt. Express* **2010**, *18*, 11700–117006. [CrossRef] [PubMed]
15. Nishizawa, N.; Andou, Y.; Omoda, E.; Kataura, H.; Sakakibara, Y. Characteristics and improvement of wideband wavelength-tunable narrow-linewidth source by spectral compression in quasi-dispersion-increasing comb-profile fiber. *Opt. Express* **2016**, *24*, 23403–23418. [CrossRef]
16. Toneyan, H.; Zeytunyan, A.; Zadoyan, R.; Mouradian, L. Classic, all-fiber, and similaritonic techniques of spectral compression. *J. Phys. Conf. Ser.* **2016**, *672*, 012016. [CrossRef]
17. Kutuzyan, A.A.; Mansuryan, T.G.; Esayan, G.L.; Akopsyan, R.S.; Muradyan, L.K. Dispersive regime of spectral compression. *Quantum Electron.* **2008**, *38*, 383–387. [CrossRef]

18. Finot, C.; Boscolo, S. Design rules for nonlinear spectral compression in optical fibers. *J. Opt. Soc. Am. B* **2016**, *33*, 760–767. [CrossRef]
19. Yi-Song, L.; Chen-Bin, H. Large-scale and structure-tunable laser spectral compression in an optical dispersion increasing fiber. *Opt. Express* **2017**, *25*, 18024–18030.
20. Chen, R.; Shi, Z.; Chang, G. Pre-Chirp-Managed Adiabatic Soliton Compression in Pressure-Gradient Hollow-Core Fibers. *Photonics* **2021**, *8*, 357. [CrossRef]
21. Li, Q.; Zhang, T.; Li, M. Spectral compression of chirp-free optical pulses in fibers with exponentially increasing dispersion. *J. Opt. Soc. Am. B* **2017**, *34*, 9. [CrossRef]
22. Szewczyk, O.; Łaszczych, Z.; Soboń, G. Spectral compression and amplification of ultrashort pulses tunable in the 1650–1900 nm wavelength range. *Opt. Laser Technol.* **2023**, *164*, 109465. [CrossRef]
23. Mouradian, L.K.; Grigoryan, A.; Kutuzyan, A.; Yesayan, G.; Sukiasyan, M.; Toneyan, H.; Zeytunyan, A.; Zadoyan, R.; Barthelemy, A. *Spectral Analogue of the Soliton Effect Compression: Spectral Self-Compressionl*; Frontiers in Optics (FIO), OSA Technical Digest; Frontiers in Optics Laser Science: Rochester, NY, USA, 2016; p. FW3F.3.
24. Grigoryan, A.P.; Kutuzyan, A.A.; Yesayan, G.L.; Mouradian, L.K. Spectral domain soliton-effect self-compression. *J. Phys. Conf. Ser.* **2016**, *672*, 12015. [CrossRef]
25. Toneyan, H.; Sukiasyan, M.; Avetisyan, V.; Kutuzyan, A.; Yeremyan, A.; Mouradian, L. *Solitonic Self-Spectral Compression of Noisy Supercontinuum Radiation*; Frontiers in Optics 2016, OSA Technical Digest; Frontiers in Optics Laser Science: Rochester, NY, USA, 2015; p. JW4A.44.
26. Akhmanov, S.A.; Vysloukh, V.A.; Chirkin, A.S. *Optics of Femtosecond Laser Pulses*; American Institute of Physics: College Park, MD, USA, 1992.
27. Sukiasyan, M. Spectral Self-Compression of partially coherent pulses. *Armen. J. Phys.* **2019**, *12*, 113–118.
28. Hardin, R.; Tappert, F. Applications of the Split-Step Fourier Method to the Numerical Solution of Nonlinear and Variable Coefficient Wave Equations. *Cronicle* **1973**, *15*, 423.
29. Fisher, R.; Bischel, W. The role of linear dispersion in plane-wave self-phase modulation. *Appl. Phys. Lett.* **1973**, *23*, 661–663. [CrossRef]
30. Kutuzyan, A.; Avetisyan, V.; Kalashyan, M.; Sukiasyan, M. *Formation of a New Type of Self-Similar Pulses in Optical Fibers with Anomalous Dispersion*; Frontiers in Optics Laser Science: Rochester, NY, USA, 2022; p. JTu4B.32.
31. Gražulevičiūtė, I.; Skeivytė, M.; Keblytė, E.; Galinis, J.; Tamošauskas, G.; Dubietis, A. Supercontinuum generation in YAG and Sapphire with picosecond laser pulses. *Lith. J. Phys.* **2015**, *55*, 110–116. [CrossRef]
32. Galinis, J.; Tamošauskas, G.; Gražulevičiūtė, I.; Keblytė, E.; Jukna, V.; Dubietis, A. Filamentation and supercontinuum generation in solid-state dielectric media with picosecond laser pulses. *Phys. Rev. A* **2015**, *92*, 33857. [CrossRef]
33. Dubietis, A.; Tamošauskas, G.; Šuminas, R.; Jukna, V.; Couairon, A. Ultrafast supercontinuum generation in bulk condensed media. *Lith. J. Phys.* **2017**, *57*, 113–157. [CrossRef]
34. Cheng, S.; Chatterjee, G.; Tellkamp, F.; Ruehl, A.; Miller, R.J.D. Multi-octave supercontinuum generation in YAG pumped by mid-infrared, multi-picosecond pulses. *Opt. Lett.* **2018**, *43*, 4329–4332. [CrossRef]